Hindawi
International Journal of Chemical Engineering
Volume 2022, Article ID 6799201, 12 pages
https://doi.org/10.1155/2022/6799201

Research Article

Volute Optimization Based on Self-Adaption Kriging Surrogate Model

Fannian Meng, Ziqi Zhang, and Liangwen Wang

Henan Key Laboratory of Intelligent Manufacturing of Mechanical Equipment, Zhengzhou University of Light Industry, Zhengzhou 450002, China

Correspondence should be addressed to Fannian Meng; mengfannian123@163.com

Received 1 July 2022; Revised 15 November 2022; Accepted 21 November 2022; Published 1 December 2022

Academic Editor: Vikranth Kumar Surasani

Optimizing the volute performance can effectively improve the efficiency of a centrifugal fan by changing the volute geometric parameter, so the self-adaption Kriging surrogate model is used to optimize the volute geometric parameter. Firstly, volute radius R_d, the radius of tongue r, and outlet angle of the volute θ are selected as the optimization parameters of the volute, and latin hypercube sampling is used to configure the initial sample points, the corresponding three-dimensional aerodynamic model under each sample point configuration is constructed. CFD software is used to simulate the aerodynamic efficiency and total pressure of the centrifugal fan under each initial sample point configuration. Secondly, the Kriging surrogate model of initial sample point configuration parameters, aerodynamic efficiency, and total pressure of volute is constructed, and sample points are added by expectation improvement (EI) method to improve the fitting accuracy of Kriging surrogate model. Finally, the high-precision Kriging surrogate model is used as the fitness function of NSGA-II algorithm to find the Pareto optimal solution under multiobjective optimization, and the optimization target are aero dynamical efficiency and total pressure. The rationality of the above method is verified by optimizing the 9–19.4A type centrifugal fan volute. The efficiency of the optimized fan under working conditions is increased by 1%, and the total pressure under working conditions is not reduced. The optimized volute can effectively improve the overall performance of the centrifugal fan. This study is helpful to promote the application of numerical optimization design method in the volute of centrifugal fan. It provides reference for the optimization design of high-performance centrifugal fan.

1. Introduction

The function of the volute is to collect and guide the gas leaving the impeller, gradually reduce the airflow speed, and turn part of the kinetic energy into static pressure. At present, domestic and foreign scholars have conducted a lot of research on centrifugal fan optimization. Zhou et al. [1] proposed a latin hypercube sampling method combined with the surrogate model to parameterize the blade profile of centrifugal fan, and multiobjective optimization is carried out under NSGA-II algorithm. Selvaraj et al. [2] optimized a centrifugal fan with the blade inlet angle, impeller diameter, and width of centrifugal fan as optimized parameters using orthogonal experimental design method. Zhou et al. [3] studied a CST function to parameterize the blade, and the surrogate model combined with the NSGA-II algorithm is used for multiobjective optimization, which provides a new idea for fan energy saving. Fan et al. [4] researched a centrifugal fan optimization method, and the hub outlet angle of impeller, the impeller outlet angle increment, the wrap angle, the hub outlet angle of the diffuser, and the diffuser outlet angle increment are set as the optimal parameters to optimization. Khalkhali et al. [5] proposed that neural network and CFD technology are used to optimize the following parameters of backward centrifugal fan: leading-edge angle, trailing-edge angle, and the stagger angle. Li et al. [6] proposed a multiobjective genetic algorithm to optimize the blade outlet installation angle and the number of blades. Finally, the compression ratio of the impeller at the design working point is increased by 3.57%, the isentropic efficiency

is increased by 0.79%, and the overall condition of the impeller is improved. Ding et al. [7] researched the influence of the blade outlet angle on the flow field in a centrifugal fan. Bamberger et al. [8] used an evolutionary algorithm combined with surrogate model to quickly optimize the geometric parameters of the centrifugal fan. Based on the adaptive Kriging surrogate model, Yu et al. [9] used the adaptive Kriging agent model to realize the geometric parameterization of the blade profile, and combined with the CFD performance solution, established the blade profile optimization design method. Based on Latin hypercube sampling and the radial basis function neural network surrogate model, Xiao et al. [10] proposed a multiobjective and multicondition constrained aerodynamic optimization design method for fuel cell air compressor impeller.

The above research mainly focuses on impeller parameter optimization; besides, the volute is also researched by some scholars, for example, Benchikh Le Hocine et al. [11] optimized the impeller and volute of the centrifugal fan, and the latin hypercube sampling and agent model are used to improve the hub shape; the efficiency is increased by 8.46%. Zhou et al. [12] improved the volute shape by improving the profile of the volute of the centrifugal fan, and the noise of the improved fan is less. Dorogokupets and Frantskevich [13] used CFX software to optimize the flow channel of centrifugal fans to improve noise performance. Huang and Tseng [14] used the Levenberg–Marquardt method and inverse design technology in determining the optimal shape of the volute spiral case for a centrifugal fan. Li et al. [15] researched the vortex characteristics of a centrifugal fan near the volute outlet region. Based on the optimization of volute profile, the orthogonal experimental design method is adopted to couple the three factors of volute width, volute tongue clearance, and relative axial position of the impeller, and the experimental scheme is determined through the orthogonal table. Using fluent numerical simulation software, the three-dimensional flow field inside the fan of some test schemes is numerically simulated and compared. The optimized total pressure and efficiency are greatly improved [16]. Zhang et al. [17] used the orthogonal experimental design method to carry out the orthogonal experimental design on the outlet expansion angle, volute tongue radius, and volute tongue clearance of the volute, established the Kriging approximate model between the air volume and the three parameters of the volute, and optimized the approximate model with genetic algorithm to obtain the optimal volute parameters. Through the simulation experiment of the optimized volute, the air volume is increased by 19.683%. At the same time, compared with the distribution of parameters such as internal speed and total pressure of the fan before and after optimization, the optimized internal speed distribution of the volute is more reasonable, and the flow loss at the volute tongue is smaller. The optimization method of volute provides an effective reference for improving the performance of the centrifugal fan. Zhou and Li [12] modified the type-line shape of the volute by introducing a dynamic moment correction coefficient to optimize the centrifugal fan. Wang et al. [18] used the grouping design model to design the impeller, volute, and volute tongue of the multiwing centrifugal fan. The design efficiency of the improved multiwing centrifugal fan was increased by 4.33%. Jiang et al. [19] introduced the response surface method into the numerical simulation of the fan volute to optimize the volute design. The calculation results show that after optimization, the static pressure of the fan is increased by 5.3%, the efficiency is increased by 4.6%, the velocity distribution in the impeller channel is more uniform, and the vortex area is significantly reduced.

The aerodynamics optimization of centrifugal fans has been studied from different perspectives in the above literatures. In this paper, the latin hypercube sampling design method combined with the self-adaption Kriging surrogate model is used to optimize the centrifugal fan volute radius R_d, radius of tongue r, and outlet angle of the volute θ. The response value is calculated by aerodynamics software CFX, and the NSGA-II algorithm is used to find the Pareto optimal volute parameter; after optimization, the airflow distribution in the volute is smoother. Engineering optimization problems have also received extensive attention in other fields, such as manufacturing [20, 21].

2. Volute Optimization Problem Descriptions

The general mathematical model of the volute optimization problem can be described as follows:

$$\begin{aligned} &\text{find}\mathbf{x} = (x_1, x_2, \cdots, x_n) \\ &\min f(\mathbf{x}) \\ &\text{s.t.} g_j(\mathbf{x}) \le 0 \\ &\mathbf{x}^{\text{LB}} \le \mathbf{x} \le \mathbf{x}^{\text{UB}} \\ &j = 1, 2, \cdots, m \end{aligned}, \tag{1}$$

where $\mathbf{x}$ is the n dimensions vector of design variable vector, $\mathbf{x}^{\text{LB}}$ and $\mathbf{x}^{\text{UB}}$ are upper and lower bounds value for design variable, respectively, f is the objective function, and g_j is the constraint condition. The analysis model for volute optimization can be described as a black-box model.

To cut down calculation cost to improve optimization efficiency, the surrogate model usually takes the place of the mathematical model. In this case, the optimization model can be described as follows:

$$\begin{aligned} &\text{find}\mathbf{x} = (x_1, x_2, \cdots, x_n) \\ &\min \hat{f}(\mathbf{x}) \\ &\text{s.t.} \hat{g}_j(\mathbf{x}) \le 0 \\ &\mathbf{x}^{\text{LB}} \le \mathbf{x} \le \mathbf{x}^{\text{UB}} \\ &j = 1, 2, \cdots, m \end{aligned}, \tag{2}$$

where $\hat{f}$ and $\hat{g}_j$ are the surrogate model approximate response value, Kriging model, radial basis function (RBF) model, support vector machine (SVM) model, deep learning machine (DLM) model, and so on, which are usually used as a surrogate model.

The air volume and total pressure (T_p) are used to ensure the gas delivery of the centrifugal fan. In the CFX centrifugal fan simulation, the air volume has been determined in the initial boundary condition settings and the total pressure value is obtained after CFX calculation, so the pressure value is one optimization target. Centrifugal fan is one kind of high energy consumption equipment. Improving efficiency is of great significance for energy conservation and emission reduction. Therefore, aerodynamic efficiency is another optimization goal. So total pressure and aerodynamic efficiency are two optimization objectives in the operation of centrifugal fans. Since the total pressure and efficiency of centrifugal fan are both interrelated and conflicting, it is difficult to achieve the optimal value of both objectives. In the paper, the multiobjective NSGA-II algorithm is employed to optimize the total pressure and efficiency of the centrifugal fan and obtain the Pareto optimal solution. The volute optimization model be described as follows:

$$\begin{aligned} &\text{find}\mathbf{x} = (R_d, r, \theta), \\ &\max \text{Eff}(\mathbf{x}), T_{\text{p}}(\mathbf{x}), \\ &\text{s.t.} R_d^{\text{LB}} \le R_{\text{d}} \le R_d^{\text{UB}}, \\ &r^{\text{LB}} \le r \le r^{\text{UB}}, \\ &\theta^{\text{LB}} \le \theta \le \theta^{\text{UB}}, \end{aligned} \tag{3}$$

where R_{d} is the volute radius, r is the radius of tongue, θ is the outlet angle of the volute, and $\text{Eff}(x)$ and $T_{\text{p}}(\mathbf{x})$ are the surrogate model approximate response values for efficiency and total pressure, respectively, and the values are calculated using self-adaption Kriging model method.

In the volute optimization process, the mathematical relation equation between the volute shape and aerodynamic response value can't be directly constructed; fortunately, computational fluid dynamics (CFD) software can be used to calculate the aerodynamic response value with geometric volute shape, but CFD calculation is time-consuming, so surrogate mode can be used in respect to CFD calculation to save time; high precision surrogate model relies on adding sufficiency sample point, so the self-adaption sample point adding method is used to improve the surrogate model fitting accuracy. In the article, the self-adaption Kriging model is used to set as an objection function to optimize. The general research method is shown in Figure 1.

3. Basic Theory Used in the Article

3.1. Latin Hypercube Sampling (LHS) Method. In m dimensions space, each one-dimension coordinate interval is divided into n small intervals, and n sample points are randomly taken in all regions; the model randomly choosing n LHS sample points in m dimensions design space is shown as follows:

$$X_{ij} = \frac{\left[r_j(i) - U_{ij}(0,1)\right]}{n}; 1 \le i \le n, 1 \le j \le m, \tag{4}$$

where $r(i)$ is the random integer permutation from 1 to n and $U(0,1)$ is the random distribution in interval $[0,1]$.

In LHS, the probability of each sample point being taken is the same, so the LHS method owns the advantages of high sampling efficiency and good uniformity. So the LHS is used to design volute geometric parameters sample points.

3.2. The Basic Kriging Model. The Kriging model can be expressed in the following equation:

$$y(x) = f(x)\beta + z(x), \tag{5}$$

where $y(x)$ is an unknown Kriging model, $fy(x)y(x)f(x)$ is known as the two order regression function of x, the global approximation model in the design space is provided, β is the undetermined coefficient of the regression function, whose value can be estimated by the known response value, and $z(x)$ is a stochastic process, it is a local deviation based on global simulation, the expectation is 0, and the variance is σ^2; the covariance matrix can be expressed as follows:

$$\text{Cov}\left[\mathbf{Z}(x_i), \mathbf{Z}(x_j)\right. = \sigma^2 \mathbf{R}\left[R\left(\mathbf{x}_i, \mathbf{x}_j\right)\right], \tag{6}$$

where R is the correlation matrix, $R(\mathbf{x}_i, \mathbf{x}_j)$ represents the correlation function of any two sample points $i, j = 1, 2, \cdots, n$, and n is the number of data in the sample. $R(\mathbf{x}_i, \mathbf{x}_j)$ has a variety of functional forms that can be selected; common correlation functions include cubic function, gauss function, linear function, spherical function, and spline function:

$$R\left(\mathbf{x}_i, \mathbf{x}_j\right) = \exp\left(-\sum_{k=1}^{n_v} \theta_k \left|x_i^k - x_j^k\right|^2\right), \tag{7}$$

where θ_k is an anisotropy parameter.

Prediction response value and prediction standard deviation at prediction point x^0, respectively, are as follows:

$$\hat{y}\left(x^0\right) = \hat{\mu} + \mathbf{r}^{\text{T}}\mathbf{R}^{-1}(\mathbf{Y} - \mathbf{F}\hat{\mu}), \tag{8}$$

$$\hat{s}^2\left(x^0\right) = \hat{\sigma}^2\left[1 - \mathbf{r}^T\mathbf{R}^{-1}\mathbf{r} + \frac{\left(1 - \mathbf{F}\mathbf{R}^{-1}\mathbf{r}\right)^2}{\mathbf{F}^{\text{T}}\mathbf{R}^{-1}\mathbf{F}}\right], \tag{9}$$

where $\hat{\mu} = (\mathbf{F}^{\text{T}}\mathbf{R}^{-1}\mathbf{F})^{-1}\mathbf{F}^T\mathbf{R}^{-1}\mathbf{Y}$, $\mathbf{Y}$ is sample point set $\hat{\sigma}^2 = (\mathbf{Y} - \mathbf{F}\hat{\mu})^{\text{T}}R^{-1}(\mathbf{Y} - \mathbf{F}\hat{\mu})/n$, and $\mathbf{F}$ is the unit column vector.

3.3. Self-Adaption Optimization Mechanism. Based on the Kriging model and EI improving critical, the self-adaption optimization algorithm takes the value at the untested point of target function as variable obeying normal distribution $\hat{y}(x) \sim N(\overline{y}(x), s(x))$, and the mean $\overline{y}(x)$ and variance $s(x)$ can be gotten from the Kriging model (from the formulas (6) and (7)), EI adding new sample point is shown as follows:

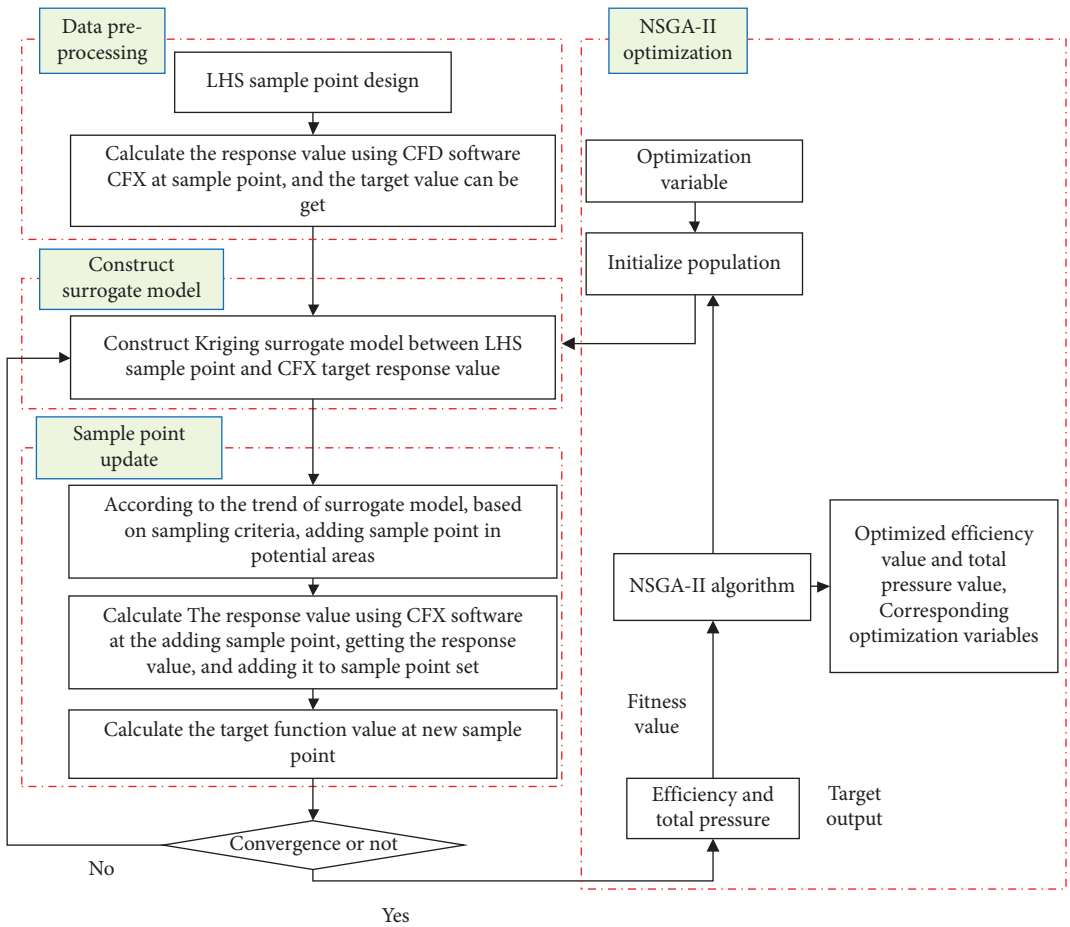

Figure 1: Self-adaption surrogate model optimization process.

$$E[I(x)] = (y_{\min} - \overline{y}(x))\Phi\left(\frac{y_{\min} - \overline{y}(x)}{s(x)}\right) + s(x)\Psi\left(\frac{y_{\min} - \overline{y}(x)}{s(x)}\right), \tag{10}$$

where $y_{\min}$ is the minimum value of target function at current experimental points, $\overline{y}$ and $s(x)$ are the prediction mean and variance of Kriging model, respectively, $\Phi(\bullet)$ and $\psi(\bullet)$ are the density function and distribution function of normal distribution, respectively. The message can be gotten from formula (8) that the prediction precision is small when the EI value is large, so the point at large EI value is stetted as a new adding sample point. The self-adaption Kriging surrogate model optimization algorithm [22] is shown in Algorithm 1.

3.4. NSGA-II Algorithm. NSGA-II is a fast nondominated multiobjective optimization algorithm and it is based on Pareto optimal solution.

Pareto domination relation: for the minimization multiobjection optimization problem and the n target components $f_i(x), i = 1, \cdots, n$, for any given two decision variables, if the following two conditions are true, it is called X_a dominates X_b.

(1) For $\forall i \in 1, 2, \cdots, n$, $f_i(X_a) \leq f_i(X_b)$ is always established

(2) $\exists i \in 1, 2, \cdots, n$, let $f_i(X_a) < f_i(X_b)$ be established

If there are no other decision variables that can dominate one decision variable, the decision variable is called the nondominated solution.

Pareto rank: in one group of solutes, the Pareto level of nondominated solution is defined as 1, and the nondominated solutes are deleted from the solution set; the Pareto level of the remaining solutions is defined as 2, and so on, so the Pareto level of all solutions in the solution set can be obtained. NSGA-II basic program is shown in Figure 2.

3.5. CFX Simulation Method. Solving the three-dimension Reynolds average Navier–Stokes equations using CFX software, specific technical steps and methods of CFD numerical simulation are shown in Figure 3.

The aerodynamics performance parameter and internal flow field can be obtained. Because the Mach number in the

Require: Initial volute geometric structure parameter sample point (**X**, **y**)
Ensure: Optimal solution $(x_{\max}, y_{\max})$
(1) **While** failure to meet shutdown criteria **do**
(2) Using the sample point aggregate (**X**, **y**) to construct Kriging surrogate model
(3) $x^{(u)} = \text{argmaxEI}(x)$
(4) Calculate the true objective value $y(x^{(u)})$ of renewal point $x^{(u)}$
(5) $\mathbf{X} \leftarrow \mathbf{X} \bigcup x^{(u)}$
(6) $\mathbf{y} \leftarrow \mathbf{y} \bigcup y(x^{(u)})$
(7) $y_{\max} \leftarrow \max(y)$
(8) $x_{\max} \leftarrow x \in \mathbf{X}$: $y(x) = y_{\max}$
(9) **end while**

Algorithm 1: Self-adaption Kriging surrogate model optimization algorithm.

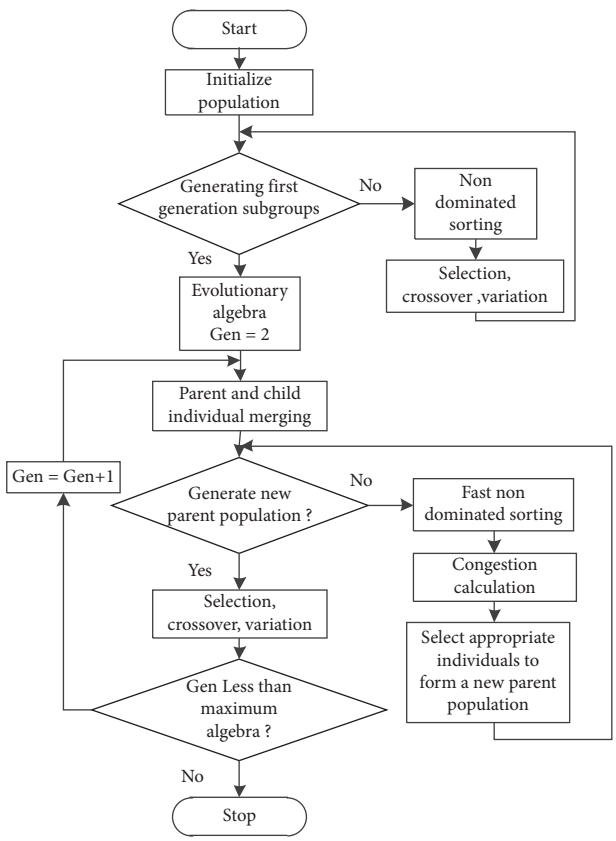

Figure 2: NSGA-II basic program.

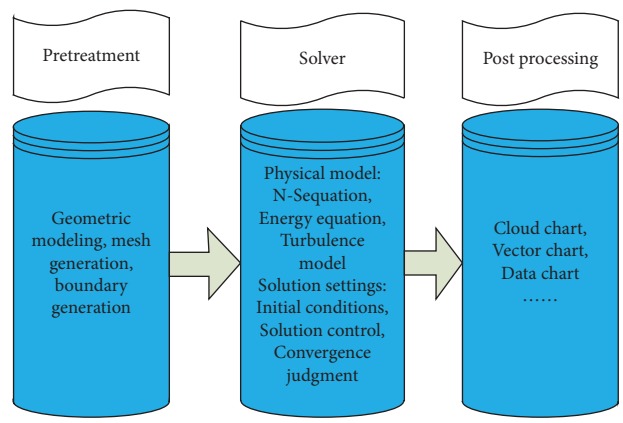

Figure 3: Technical steps and methods of CFD numerical simulation.

centrifugal fan is less than 0.3, so the internal flow in the centrifugal fan can be regarded as the incompressible gas, $k-\varepsilon$ model is used as turbulence model, high-resolution scheme is adopted for convection term, and second-order central scheme is used for the viscous term. CFD calculation parameter setting is shown in Table 1.

In order to set the boundary conditions conveniently, the inlet and outlet sections of the centrifugal fan are extended appropriately, the total pressure is set as inlet boundary, and the mass flow rate is set as an outlet boundary condition, the wall satisfies the nonslip boundary condition, rotor–stator interactional surface is dealt with multiple reference frame method, the static coordinate system is adopted in the entrance and volute region, and the rotating coordinate system is adopted in the impeller region.

4. Volute Optimization Analyses

4.1. Centrifugal Fan Structure. Collector, impeller, and volute are the main parts of the centrifugal fan; the task of the volute is to guide the gas leaving the impeller to the outlet of the volute and changing parts of the dynamic pressure into static pressure. The overall structure of the centrifugal fan and volute structure are shown in Figure 4.

4.2. CFD Simulation Analysis. In order to calculate the aerodynamic response parameters under a specific centrifugal fan model, CFD software needs to be used for numerical simulation calculation. Here, $^{*}x\_t$ model parameters are imported into ICEM software to divide the grid. The divided grid is shown in Figure 5.

Grid sparsity and quality affect the accuracy of CFD calculation. In order to improve the accuracy of simulation calculation, grid independence trial calculation is used to analyze the influence of grid sparsity on calculation results. Grid independence trial calculation is shown in Figure 6.

Table 1: CFD calculation parameter setting.

Term	Setting
Turbulence model	$k-\varepsilon$ model
Convection term	High resolution scheme
Viscous term	Second-order central scheme
Time derivative term	Second-order backward scheme

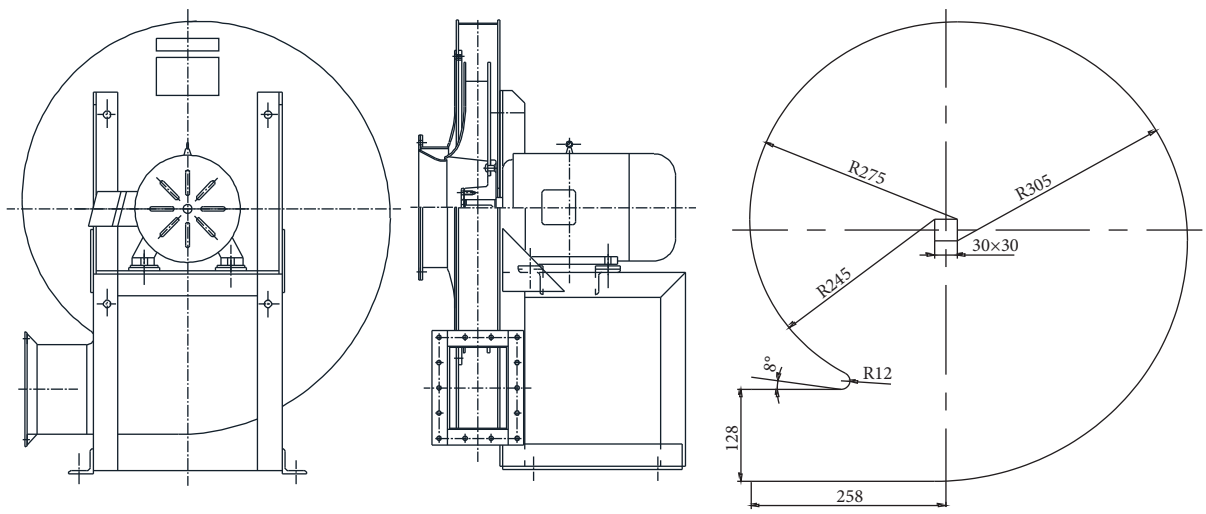

(a) (b)

Figure 4: Centrifugal fan structure: (a) overall structure and (b) volute structure.

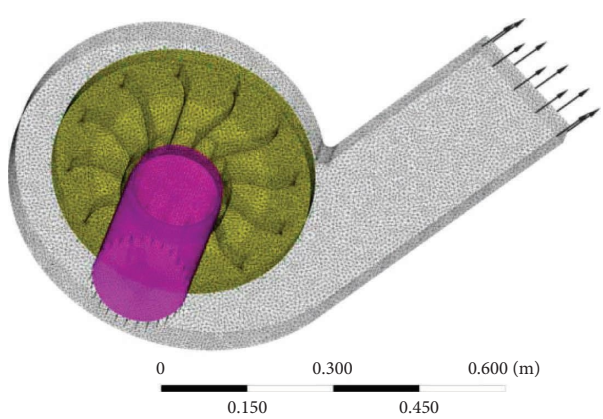

Figure 5: Grid mesh.

4.3. Efficiency and Total Pressure Calculation. The calculation equations of total pressure (T_p) and efficiency (Eff) are shown as follows:

$$T_p = P^*_{out} - P^*_{in}, \tag{11}$$

where P^*_{out} is the outlet total pressure, Pa and P^*_{in} is the inlet total pressure, Pa.

The Eff is defined as follows:

$$\text{Eff} = \frac{T_p \times Q}{W \times 3600}, \tag{12}$$

where Q is the volume flow, m^3/h and W is the shaft power, W.

4.4. Sample Point Design. First, volute radius R_d, radius of tongue r, and outlet angle of the volute θ are selected as optimization parameters. Eff and T_p are selected as an objective parameter. That is to say, there are three factors to consider in the optimization process. The initial volute radius parameter is equal to 235 mm. On this basis, it floats 10 mm upward and 10 mm downward, and the value range of volute radius is from 235 mm to 255 mm. Besides, the initial radius of tongue is equal to 12 mm. Similarly, it floats 4 mm upward and 4 mm downward, respectively. The value range of the radius of tongue is from 8 mm to 16 mm. The initial outlet angle of the volute is 0°, and it is increased by 10° upwards, so the outlet angle of the volute is from 0° to 10°. The factors and their levels are listed in Table 2.

According to the optimization problem, the multi-objective optimization can be written as follows:

$$\begin{cases} \max \text{Eff}\left(R_d, r, \theta\right) \\ \max T_p\left(R_d, r, \theta\right) \end{cases} \begin{cases} 235 \le \text{Rd} \le 255 \\ 8 \le r \le 16 \\ 0^\circ \le \theta \le 10^\circ \end{cases}. \tag{13}$$

In this research, the LHS method is used to design parameters. Based on the LHS theory, an array with ten rows is used for the simulation experiments. The numerical simulation results are listed in Table 3 and Figure 7.

It is obvious that the distribution of sample points in each region of subspace is relatively uniform. The sample points also show a uniformly distributed full coverage state in the subspace formed by other factors.

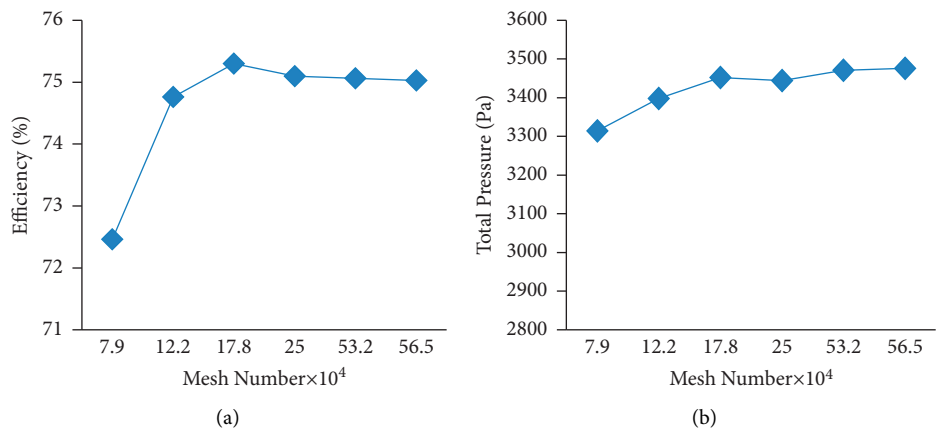

Figure 6: Grid independent calculation: (a) efficiency and (b) total pressure.

Table 2: CFD calculation parameter setting.

Factors	Parameters	Range
A	Volute radius R_d	235~255
B	Radius of tongue r	8~16
C	Outlet angle of the volute θ	0~10

Table 3: Self-adaption Kriging surrogate model optimization algorithm.

Number	Volute radius R_d	Radius of tongue r	Outlet angle of the volute θ
1	254	15.6	7.5
2	244	13.2	0.5
3	248	11.6	1.5
4	240	10.8	5.5
5	236	14	2.5
6	252	10	3.5
7	246	9.2	8.5
8	250	12.4	4.5
9	242	8.4	6.5
10	238	14.8	9.5

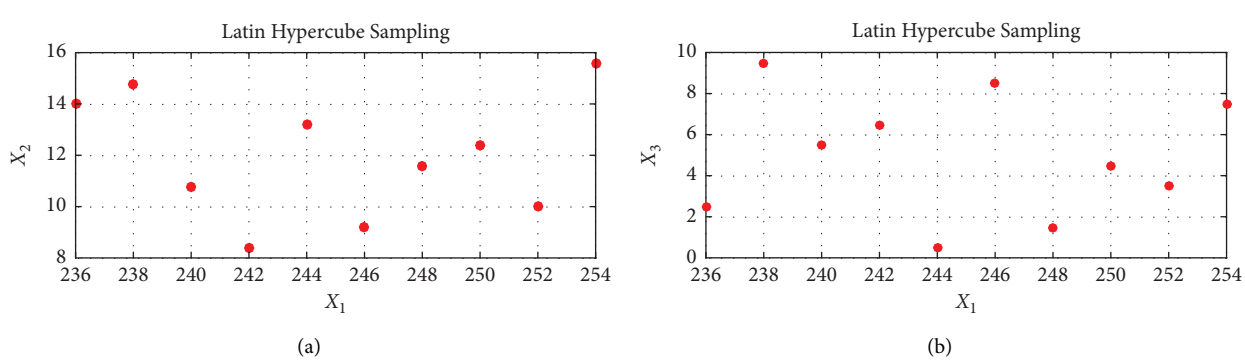

Figure 7: Latin hypercube sampling.

It can be seen from the left figure of Figure 7(a) that at position 236, 238, 240, 242, 244, 246, 248, 250, 252, and 254 of x_1, one sample point is distributed at each position. Similarly, at position 8.4, 9.2, 10, 10.8, 11.6, 12.4, 13.2, 14, 14.8, and 15.6 of x_2, one sample point is also distributed at each position. Similarly, the right figure of Figure 7(b) also

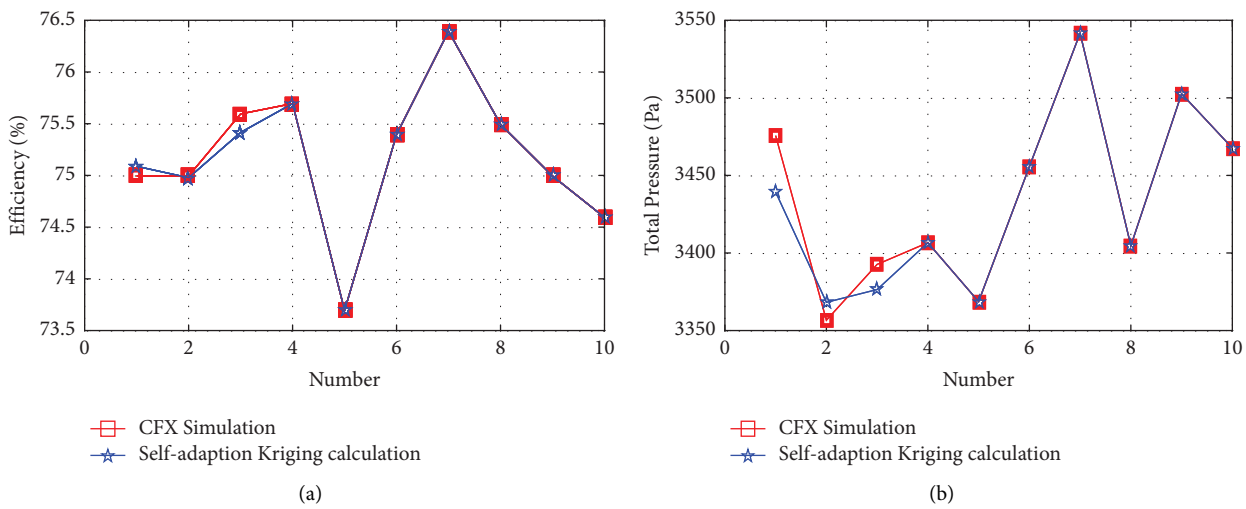

Figure 8: The output response value calculated by CFX simulation and self-adaption Kriging method: (a) efficiency and (b) total pressure.

follows this rule. This rule is the characteristic of LHS method, which ensures the uniformity of sample point distribution.

The corresponding model of each sample point is calculated by CFD simulation and self-adaption Kriging method, and the output response parameters fan efficiency and total pressure obtained are shown in Figure 8. It can be seen from Figure 8 that the CFX simulation results are in good agreement with the results of the self-adaption Kriging model, indicating that the accuracy of the self-adaption Kriging model meets the accuracy requirements.

4.5. Self-Adaption Adding Point Result Comparison. Sufficient sample points can directly affect the fitting precision of the surrogate model; in order to improve the fitting precision of the surrogate model, sample points adding method is used to ensure the precision of the surrogate model. Figure 9 shows the relative fitting error before and after adding points.

It can be seen from the Figure 9 that it is significantly improved after optimization for the fitting accuracy of the efficiency.

4.6. NSGA-II Algorithm Optimization. NSGA-II Algorithm is used for optimization and the parameters are set as: maximum evolutionary algebra, 300; population size, 100; crossover probability, 0.9; variation probability, 0.1; scaling factor, 0.5; and the distribution index of crossover and mutation algorithm, 20. The optimal combination of optimization parameters is calculated. After the combination of the parameters is rechecked by CFD, the total pressure error of the fan is 0.5% and the efficiency error of the fan is 0.1%, indicating that the response surface accuracy is high and the result is reliable. The fan efficiency is increased by 0.9%. The distribution of nondominated solution set is shown in Figure 10.

Table 4 shows the comparison of total pressure and efficiency at the design points before and after optimization. It is known that at the design points, the total

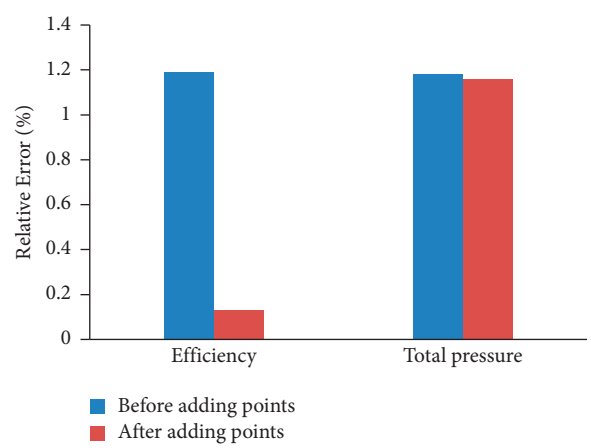

Figure 9: Relative fitting error before and after adding points.

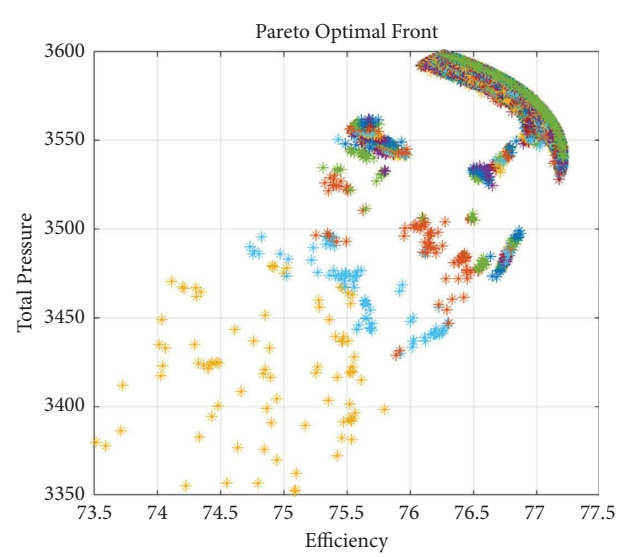

Figure 10: The distribution of nondominated solution set.

Table 4: Self-adaption Kriging surrogate model optimization algorithm.

Centrifugal fan	Total pressure at design point (Pa)	The efficiency at design point (%)
Before optimization	3538	76.3
After optimization	3545	77.2

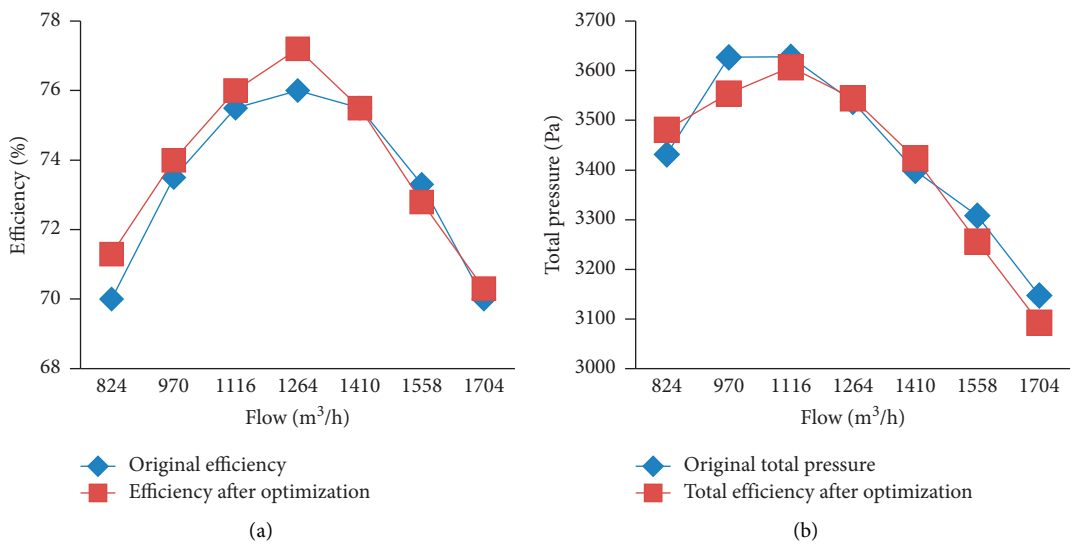

Figure 11: Performance curve before and after optimization: (a) efficiency and (b) total pressure.

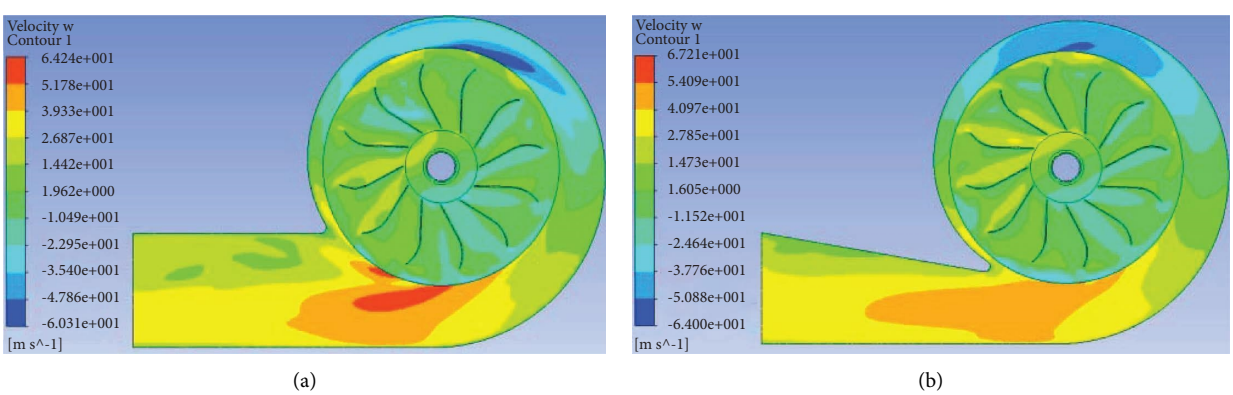

Figure 12: Velocity distribution: (a) before optimization and (b) after optimization.

pressure of the optimized fan is increased from 3538 Pa to 3545 Pa, and the efficiency is increased from 76.3% to 77.2%. The efficiency of the optimized centrifugal fan is improved under the condition that the total pressure is not lower than that of the original fan. The optimized centrifugal fan is more energy-saving and has better performance.

Although there is only 1% efficiency improvement, it can also save a lot of power for high-power equipment. For example, for a 5000 t/d cement production line, the total installed power is close to 41 MW, and the total installed power of main process fans is about 13 MW, accounting for about 1/3 of the total installed power. After the overall efficiency is increased by 1%, at least 1.5 million kilowatt hours of electricity can be saved every year, with considerable economic benefits.

4.7. Volute Internal Flow Performance Comparison before and after Optimization. Figure 11 are the performance curves before and after optimization ((a) corresponds to the efficiency curve and (b) corresponds to the total pressure curve). It is known from this that under the design conditions after optimization, the total pressure of the optimized centrifugal fan is not less than the total pressure of the original fan and its efficiency is increased by about 1%, which is of great significance for improving the performance of the whole machine.

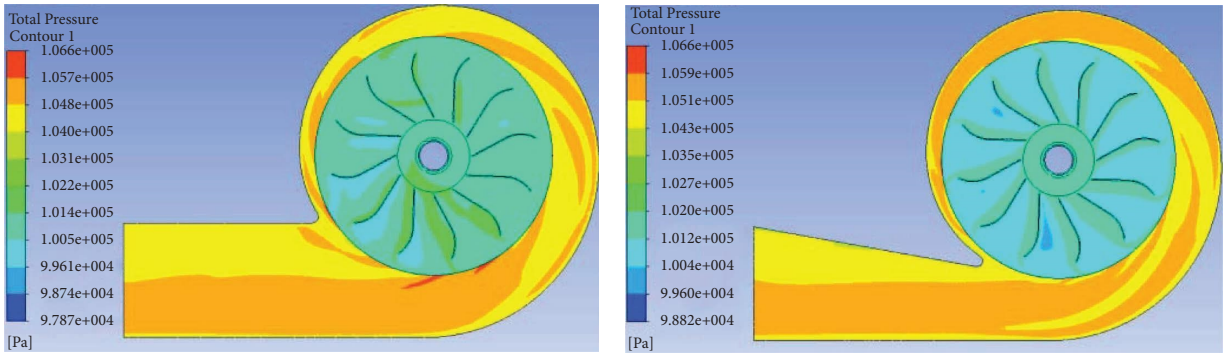

(a) (b)

Figure 13: Total pressure distribution: (a) before optimization and (b) after optimization.

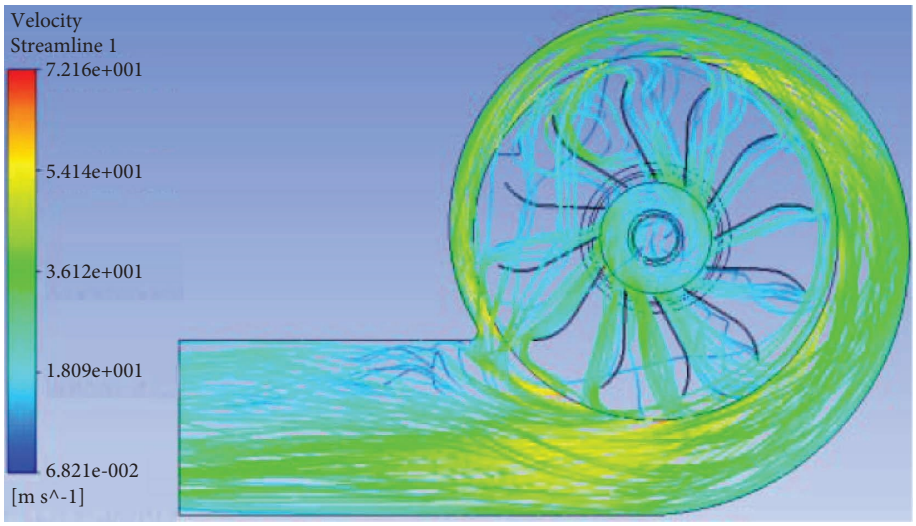

(a)

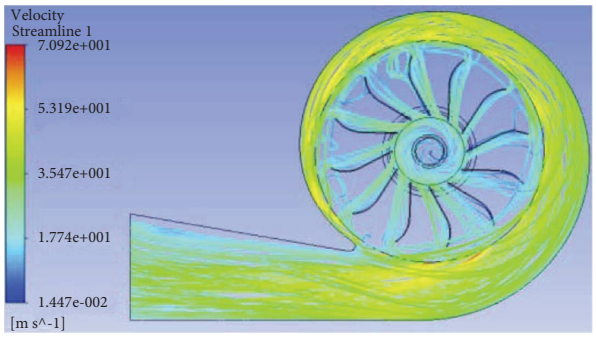

(b)

Figure 14: Velocity streamlines distribution: (a) before optimization and (b) after optimization.

Figure 12 shows the velocity distribution before and after optimization. It can be concluded from the figure that the velocity distribution in the volute after optimization is more uniform, especially in the area where the volute is in contact with the impeller.

Figure 13 shows the total pressure distribution before and after optimization. It can be concluded from the figure that the total pressure distribution in the volute after optimization is more uniform.

Figure 14 compares the streamline distribution before and after the optimization of centrifugal fan, respectively. The results show that the optimized air flow distribution is more uniform. After optimization, the overall flow in the impeller and volute becomes better. It can be seen from Figure 14(a) that there is an obvious low-speed vortex mass near the volute tongue at the outlet of the fan before optimization. After optimization, the air flow distribution near the volute tongue tends to be good as a whole, and the

velocity distribution in the volute is smoother, which is beneficial to reducing the flow loss.

5. Conclusions

In the article, the Kriging surrogate model is established, the EI adding point's method is used to improve the accuracy of the model, and the genetic algorithm is used for optimization. The volute optimization design process considering the aerodynamic performance of the centrifugal fan is proposed, and the centrifugal fan with better comprehensive performance is optimized.

(1) CFD method is complex and time-consuming to solve aerodynamic forces. The point-adding optimization method combining the Kriging model with EI point-adding optimization method can obtain a higher precision model with fewer sample points, which significantly improves the optimization efficiency.

(2) After optimizing the volute, the aerodynamic performance of the centrifugal fan is improved, and the efficiency of the integral centrifugal fan is increased by 1%.

Data Availability

The data used to support the findings of this study are available from the corresponding author upon request.

Disclosure

An earlier version of this paper was presented in Proceedings of the 1st International Conference on New Materials Machinery and Vehicle Engineering.

Conflicts of Interest

The authors declare that they have no conflicts of interest to report regarding the present study.

Acknowledgments

This paper is supported by the National Natural Science Foundation of China, (no. 52075500), by the Key Science and Technology Research Project of the Henan Province (no. 212102210071), and by Educational Commission of Henan Province (no. 21A460037).

References

[1] S. Q. Zhou, H. X. Zhou, K. Yang, H. B. Dong, and Z. L. Gao, "Research on blade design method of multi-blade centrifugal fan for building efficient ventilation based on Hicks-Henne function," *Sustainable Energy Technologies and Assessments*, vol. 43, pp. 100971.1–100971.13, 2021.

[2] T. Selvaraj, P. Hariharasakthisudhan, S. Pandiaraj, K. Sathickbasha, and N. Aslam, "Optimizing the design parameters of radial tip centrifugal blower for dust test chamber application through numerical and statistical analysis," *FME Transactions*, vol. 48, no. 2, pp. 236–245, 2020.

[3] S. Q. Zhou, K. Yang, W. T. Zhang, K. Zhang, C. H. Wang, and W. Jin, "Optimization of multi-blade centrifugal fan blade design for ventilation and air-conditioning system based on disturbance CST function," *Applied Sciences*, vol. 11, no. 17, pp. 7784.1–7784.20, 2021.

[4] H. G. Fan, J. S. Zhang, W. Zhang, and B. Liu, "Multi-parameter and multi-objective optimization design based on orthogonal method for mixed flow fan," *Energies*, vol. 13, no. 11, pp. 2819–2915, 2020.

[5] A. Khalkhali, M. Farajpoor, and H. Safikhani, "Modeling and multi-objective optimization of forward-curved blade centrifugal fans using CFD and neural networks," *Transactions of the Canadian Society for Mechanical Engineering*, vol. 35, no. 1, pp. 63–79, 2011.

[6] X. F. Li, X. Y. Yin, and G. F. Yin, "Parameter optimization of centrifugal compressor impeller based on CFD and multi-objective algorithm," *Fluid Machinery*, vol. 47, no. 3, pp. 31–36, 2019.

[7] H. C. Ding, T. Chang, and F. Lin, "The influence of the blade outlet angle on the flow field and pressure pulsation in a centrifugal fan," *Processes*, vol. 8, no. 11, pp. 1422.1–1422.14, 2020.

[8] B. Konrad, C. Thomas, B. Jujian, and N. Oliver, "Development, validation, and application of an optimization scheme for impellers of centrifugal fans using computational fluid dynamics-trained metamodels," *Journal of Turbomachinery*, vol. 142, pp. 1–7, 2020.

[9] R. Yu, D. W. Zhou, X. C. Zhu, and Z. H. Du, "Aerodynamic optimization design of airfoils based on adaptive Kriging surrogate model," *Journal of Chinese society of power engineering*, vol. 34, no. 2, pp. 103–107, 2014.

[10] J. Xiao, Y. D. Wang, X. M. Liu, Y. H. Chen, and Z. P. Zhang, "Multi-point Aerodynamic optimization of the high-speed centrifugal impeller used in the fuel-cell Vehicle," *Journal of Xi'an Jiao tong University*, vol. 55, no. 9, pp. 1–12, 2021.

[11] A. E. Benchikh Le Hocine, S. Poncet, and H. Fellouah, "CFD modeling and optimization by metamodels of a squirrel cage fan using OpenFoam and Dakota: ventilation applications," *Building and Environment*, vol. 205, pp. 108145.1–108145, 2021.

[12] S. Q. Zhou and Y. B. Li, "Volute characteristics of centrifugal fan based on dynamic moment correction method," *Proceedings of the Institution of Mechanical Engineers - Part A: Journal of Power and Energy*, vol. 233, no. 2, pp. 176–185, 2019.

[13] A. S. Dorogokupets and V. S. Frantskevich, "Optimization of flow passage of centrifugal fan of grinding-separating unit," *Chemical and Petroleum Engineering*, vol. 53, no. 5-6, pp. 390–395, 2017.

[14] C. H. Huang and W. C. Tseng, "An optimal volute spiral case design for centrifugal fan: theoretical and experimental studies," *International Journal of Mechanics and Materials in Design*, vol. 12, no. 2, pp. 223–240, 2016.

[15] Z. H. Li, X. X. Ye, and Y. K. Wei, "Investigation on vortex characteristics of a multi-blade centrifugal fan near volute outlet region," *Processes*, vol. 8, no. 10, pp. 1240.1–1240.18, 2020.

[16] B. Zhang and Y. K. Lv, "D multi-factor optimal research on centrifugal fan based on orthogonal design," *Fluid Machinery*, vol. 45, no. 6, pp. 10–15, 2017.

[17] L. Zhang, K. Huang, G. X. Huang, and B. Cheng, "Study on optimization of outlet structure of centrifugal fan volute," *Fluid Machinery*, vol. 47, no. 6, pp. 47–51, 2019.

[18] K. Wang, Y. P. Ju, and C. H. Zhang, "Design of Multi-blade centrifugal fan based on grouping model and bionic volute

tongue," *Journal of engineering thermos-physics*, vol. 38, no. 8, pp. 1671–1675, 2017.

[19] W. S. Jiang, P. Zhang, Z. L. Yang, and Q. Q. Pei, "Aerodynamic optimization of centrifugal fan for volute by response surface methodology," *Chinese journal of turbomachinery*, vol. 61, no. 6, pp. 23–28, 2019.

[20] W. Ming, J. Hou, Z. Zhang et al., "Integrated ANN-LWPA for cutting parameter optimization in WEDM Ming," *International Journal of Advanced Manufacturing Technology*, vol. 84, no. 5-8, pp. 1277–1294, 2016.

[21] W. Ming, X. Guo, Y. Xu et al., "Progress in non-traditional machining of amorphous alloys," *Ceramics International*, vol. 49, no. 2, pp. 1585–1604, https://doi.org/10.1016/j.ceramint.2022.10.349, 2022.

[22] D. W. Zhan, *Parallel EGO Algorithms and Their Applications (Doctoral Thesis)*, Huazhong University of Science and Technology, Wuhan, China, 2018.